nature microbiology

SUPPLEMENTARY INFORMATION

https://doi.org/10.1038/s41564-020-0700-6

In the format provided by the authors and unedited.

SspABCD–SspE is a phosphorothioation-sensing bacterial defence system with broad anti-phage activities

Xiaolin Xiong[1,2,5,7], Geng Wu[3,7], Yue Wei[1,7], Liqiong Liu[1,3], Yubing Zhang[1,3], Rui Su[4], Xianyue Jiang[1], Mengxue Li[1], Haiyan Gao[1,3], Xihao Tian[1], Yizhou Zhang[1,5], Li Hu[1,5], Si Chen[1], You Tang[1,5], Susu Jiang[1,5], Ruolin Huang[1,5], Zhiqiang Li[5], Yunfu Wang[2], Zixin Deng[1,3], Jiawei Wang[4], Peter C. Dedon[6], Shi Chen[1,2,5] and Lianrong Wang[1,2,5] ✉

[1]Ministry of Education Key Laboratory of Combinatorial Biosynthesis and Drug Discovery, School of Pharmaceutical Sciences, Wuhan University, Wuhan, China. [2]Taihe Hospital, Hubei University of Medicine, Shiyan, China. [3]State Key Laboratory of Microbial Metabolism, School of Life Sciences and Biotechnology, The Joint International Research Laboratory of Metabolic and Developmental Sciences, Shanghai Jiao Tong University, Shanghai, China. [4]State Key Laboratory of Membrane Biology, Beijing Advanced Innovation Center for Structural Biology, School of Life Sciences, Tsinghua University, Beijing, China. [5]Department of Neurosurgery, Zhongnan Hospital, Wuhan University, Wuhan, China. [6]Department of Biological Engineering, Massachusetts Institute of Technology, Cambridge, MA, USA. [7]These authors contributed equally: Xiaolin Xiong, Geng Wu, Yue Wei. ✉e-mail: lianrong@whu.edu.cn

Supplementary Results

SspB dimerization is required for DNA nicking

Sequence alignment of SspB revealed three conserved motifs at the N-terminus: "H^{17}ETFAPRF^{24}" (referred to as motif 1), "L^{50}GVGKNMV^{57}" (motif 2), and "D^{101}PYLEE^{106}" (motif 3) (**Extended Data Fig. 1a**). Mapping the sequence conservation of SspB onto its structure indicated that the three motifs were located adjacent to one another on the most conserved surface patch of SspB (**Extended Data Figs. 1b and 1c**). In contrast, the "back" side of the SspB surface was much less conserved (**Extended Data Fig. 1d**).

There were two molecules of SspB in the asymmetric unit in the crystal structure, and they were related by a two-fold rotation axis (**Fig. 2c**). However, SspB behaved as a monomer in solution (**Supplementary Fig. S10**). Therefore, SspB formed a pseudodimer, likely resulting from a weak dimerization interface similar to that in FokI[1]. Motif 3 and the C-terminal half of motif 1 were involved in SspB pseudodimerization (**Fig. 2d**). At the pseudodimeric interface, the positively charged guanidinium groups of R23 and R203 from one SspB molecule formed salt bridges with the negatively charged carboxyl groups of E105 and E204 from the other SspB molecule. Additionally, F24, H28, and Y103 from both SspB molecules clustered together by hydrophobic interactions (**Fig. 2d**). In addition to CCC and linear forms of dsDNA, SspB can also introduce massive breaks in ssDNA, manifested by the degradation of ϕX174 ssDNA upon treatment with SspB (**Supplementary Fig. S11**). However, SspB still exerted nickase activity in a non-sequence-specific manner even in the presence of SspC, which was shown to form a complex with SspB by pulldown analysis (**Extended Data Fig. 6**).

Identification of *sspE* and its involvement in growth defects of PT-deficient *Vibrio* mutants at low temperatures

A major missing piece in the comparison of *dnd* and *ssp* systems is the restriction activity of DndFGH. Upon the deletion of *dndBCDE*, genomic DNA without PT protection is susceptible to dsDNA cleavage by DndFGH, which then triggers the SOS response, cell filamentation and prophage gene induction[2,3]. We used this approach to knock out *sspBCD* modification genes to identify possible restriction activity in *V. cyclitrophicus* FF75 by virtue of toxic DNA cleavage. The Δ*sspBCD* and the individual *sspABCD* deletion mutants had the same growth behavior as wild-type cells at 28 °C, with no obvious signs of toxicity, suggesting the lack of classical restriction activity in FF75 (**Extended Data Fig. 7a**). However, since FF75 is a psychrotolerant marine

bacterium capable of growing at 4 °C, we assessed the growth of the mutants at low temperatures and found severe growth defects at both 15 °C and 4 °C compared to wild-type growth (**Extended Data Fig. 7a**).

This unusual behavior motivated a search for proteins mediating the temperature-dependent growth inhibition of FF75. We performed a quantitative proteomic comparison of wild type and the single-gene deletion mutant Δ*sspC*, which lacks PT. The growth defects of the mutant cells at low temperatures necessitated using 22 °C as the restrictive temperature, which allowed enough cell growth for analysis relative to normal growth at 28 °C. Comparison of the iTRAQ proteomic profiles of Δ*sspC* and wild-type FF75 grown at 22 °C and 28 °C immediately revealed that one protein, M565_ctg1P1910, showed the largest downregulation in ΔsspC at 28 °C (reduced by 0.72-fold) (**Supplementary Data 1**).

Located immediately downstream of *sspD*, the *M565_ctg1P1910* gene encodes a 785-amino-acid protein harboring two domains of unknown function, DUF262 and DUF1524 (**Fig. 1b**). Two lines of evidence confirmed the involvement of M565_ctg1P1910 in the temperature-dependent growth arrest of PT-deficient *Vibrio* mutants. First, the double-deletion mutant Δ(*sspBCD*, *ctg1P1910*) grew normally, similar to FF75, at all temperatures, including 15 °C and 4 °C, which normally resulted in growth inhibition for Δ*sspBCD* (**Extended Data Fig. 7a**). Second, quantitative real-time PCR (qPCR) and Western blot analyses revealed that M565_ctg1P1910 abundance was thermoregulated, with enhanced transcription and expression at 15 °C compared to those at 28 °C, in agreement with the observed growth defect of PT-deficient *Vibrio* mutants at low temperatures (**Extended Data Figs. 7b and 7c**). Considering this functional relationship between *M565_ctg1P1910* and the *sspABCD*-dependent PT modification system, we designated *M565_ctg1P1910* as *sspE*.

It is noteworthy that this temperature-dependent lack of growth in the PT-deficient *Vibrio* mutants was not due to massive cell death, with cell viability assays showing no apparent loss of viability in the mutant cells when cultures grown at 28 °C (~0.5 OD_{600}) were shifted to 15 °C (**Extended Data Fig. 7d**). This established that the growth defect mediated by SspE is attributed to a shift to a slow- or nongrowing phenotype rather than massive cell death, which agreed well with the increased tolerance of Δ*sspBCD* mutant cells towards two bactericidal antibiotics, ampicillin and streptomycin; these antibiotics typically eradicate actively replicating cells by disrupting essential and active targets (**Extended Data Fig. 7e**).

The phylogenetic distribution of Ssp systems

Using the FF75 SspBCD-SspE amino acid sequences as queries to perform a BLAST search against the NCBI databases as previously described[4], we found SspBCD-SspE homologs in 234 bacterial strains representing diverse species and habitats (**Supplementary Data 2**). By concatenating the homologs of SspBCD-SspE in each strain, we constructed the maximum-likelihood tree of SspBCD-SspE using MEGA 5.2 (**Extended Data Fig. 3**). Although the topology of the tree largely matched the corresponding species tree, several exceptions were found, indicating potential horizontal gene transfer events. For example, *Pseudomonas syringae* CC1629 was grouped with *Xanthomonas* and *Burkholderia* instead of with other *Pseudomonas* strains. A similar situation was found for *Klebsiella*, of which two strains (*Klebsiella variicola* WUSM_KV_97 and *Klebsiella pneumoniae* EuSCAPE_RO04) were phylogenetically not grouped with the rest (**Extended Data Fig. 3**).

Structure determination of SspE

Through the SAD method using a SeMet derivative of SspE, the structure of SspE from *S. yokosukanensis* DSM 40224 was solved with a resolution of 3.31-Å (**Supplementary Table S4**). Due to the mediocre resolution of the X-ray diffraction data, only the main chains and not the side chains of the C-terminal DUF1524 domain (residues 327-771) could be resolved, while both the main chains and side chains of the N-terminal DUF262 domain (residues 1-326) could be clearly visualized. We then aligned the SspE structure with another ParB/sulfiredoxin fold-containing protein human sulfiredoxin (hSrx) (**Fig. 5c**). Two templates were used for TM-align[5]; the hSrx-ADP complex (PDB:1XW4) and the hSrx-ATP-Mg (PDB:3CYI) complex. Alignments revealed credible similarity (TM-score > 0.5), especially similar structures between IIDGQQR (SspE) and SFGGCHR (hSrx): both were part of the active pocket, while the side chain of the arginine residue was close to the β-phosphate of an ATP molecule, suggesting its role in substrate binding or phosphate bond hydrolysis.

A similar domain organization, DUF262 and DUF1524, occurs in GmrSD, a type IV modification-dependent endonuclease preferentially cleaving DNA with glucosyl-5-hydroxymethyl-cytosines (glc-5hmC)[6]. However, phage resistance assays showed that SspABCD-SspE exhibited the same antiphage activities against T4 and T4gt (T4 mutant deficient in α-, β-glucosyltransferase), regardless of their glc-5hmC DNA and nonglycosylated 5hmc DNA, respectively (**Fig. 3a**). Additionally, the nicking activity of full-length SspE *in vitro* remained unchanged despite the addition of GTP and/or synthesized C_{PS}CA-containing DNA fragments (sequences are listed in **Supplementary Table S3, Supplementary Fig. S12**), ruling out a mechanism of

ATP/GTP-stimulated REase activity akin to that of GmrSD[7]. The results suggested that despite a similar double-domain form, the two systems SspABCD-SspE and GmrSD provide protection against phages via different modes of action.

Supplementary Discussion

The unusual defense of SspE

The unusual temperature-dependent defense of SspE seems to confer a fitness advantage to FF75 by resisting phage infection in moderate-temperature environments such as soil and water. Cases of using temperature as an environmental cue to regulate defensive behaviors are rare, with a few recent reports of two R-M systems, LlaJI and LmoH7, and one CRISPR-Cas system[8-10]. LlaJI and LmoH7 R-M systems in *Lactococcus lactis* and *Listeria monocytogenes* ECII, respectively, confer phage resistance at low temperatures, while this CRISPR adaptation increases resistance with decreasing temperatures in *Pseudomonas aeruginosa*[8-10]*.*

Moreover, the PT-dependent antiphage behavior seems to be discrepant with the observation that SspE still exerts nicking activity despite the absence of PT. One plausible explanation is that the nicking endonuclease activity of SspE is PT independent but is coupled to other critical steps (discussed briefly), driven by PT-stimulated NTPase activity *in vivo* to efficiently exert toxicity. In terms of the SspE-mediated phenotypic changes in PT-deficient *Vibrio* mutants, one possible scenario may involve the balance between DNA nicking damage and repair. Given that SspE has higher expression at 15 °C than at 28 °C in FF75, one can imagine that the PT-deficient resident DNA would undergo an increase in intensive nicking damage following a downshift in temperature. However, the less-active DNA repair machinery is insufficient for the aggravating DNA nicks at low temperatures, which consequently interferes with DNA replication and impairs bacterial growth. In comparison, the fewer DNA nicks and the more active DNA repair system at the optimal growth temperature (28 °C) than at low temperatures lead to efficient repair of DNA damage, which agrees with the observation that the toxicity of SspE can be not only reversed by complementation with PTs but also relieved by a temperature rise. This also reflects the fact that SspE acts as a nicking endonuclease with weak activity. Indeed, when pUC19 was treated with SspE, the majority of the nicking products formed were OC rather than linearized DNA. Even after overnight incubation, only a small fraction of linearized DNA product was formed, which was not further intensively degraded to smaller DNA fragments with prolonged incubation.

Surprisingly, bacterial host DNA with d(C_{PS}C) modification was still susceptible to SspE nicking *in vitro* (**Supplementary Fig. S13**). This result is seemingly contradictory to the self-nonself discrimination mechanism of canonical R-M systems but is actually understandable considering the unusual PT heterogeneity in a population of bacterial cells[11,12]. The PT heterogeneity reflects two possibilities: (1) the cognate SspE behaves heterogeneously in cells, and (2) unusual target selection mechanisms occur *in vivo*. Therefore, one could envisage a scenario in which the non-PT-protected targets across the genomic DNA are no longer protected from SspE *in vitro*.

The biological relevance of the Ssp system favoring GTP, CTP, and UTP over ATP is not yet clear. Considering that Dnd systems use ATP as an effector molecule to control the expression of *dndBCDE*[13], it might be advantageous to not compete for the same cofactor if Ssp and Dnd systems coexist in the same bacterium, e.g., *Anabaena variabilis* ATCC 29413.

Strategies to evade Ssp systems

Plaque assays showed that phage T5 was capable of evading the Ssp defense regardless of the growth temperature (15 °C or 28 °C), implying that anti-Ssp mechanisms may have evolved or been acquired in some phages during the evolutionary battle with bacteria. Similar to other phages used in this study, phage T5 harbors 3,523 5'-CCA-3' motifs in its genome (**Supplementary Table S2**). The *in vitro* enzymatic assays showed that isolated T5 DNA was still susceptible to the nicking activity of SspE (**Supplementary Fig. S12**), ruling out the possibility that phage T5 escapes the defense by the Ssp system via DNA chemical modifications. During infection, T5 DNA injection occurs in an unusual two-step mechanism: 7.9% of the genome, referred to as the first step transfer (FST) sequence, first infects the host, and in the second step transfer (SST), the remainder of T5 DNA enters the host only after the expression of FST genes. The FST region is responsible for numerous properties, including the SST, the shutting off the synthesis of host macromolecules, host DNA degradation, inhibition of DNA methylation, and restriction insensitivity[14]. To date, T5 has been found to be insensitive to restriction by (at least) EcoRI, EcoK and EcoPI, despite the presence of these restriction sites on its genome[15]. Moreover, unusual features of T5 also include the existence of naturally occurring nicks at specific locations and large terminal repeats[14,16]. It would be of interest in the future to investigate whether and how these unique features or alternative anti-Ssp tactics enable phage T5 to survive the defense by the Ssp system and other REases.

Table S1. SspB structural data collection and refinement statistics

	Native SspB	Magnesium ion-bound SspB	SeMet-SspB
Data collection			
Space group	$P2_12_12_1$	$P2_12_12_1$	$P2_12_12_1$
Cell dimensions			
a, *b*, *c* (Å)	57.40, 81.64, 148.0	57.25, 80.25, 146.02	57.51, 81.54, 148.02
α, β, γ (°)	90, 90, 90	90, 90, 90	90, 90, 90
Wavelength	0.97893 Å	0.97893 Å	0.97893 Å
Resolution (Å)	50-1.59 (1.62-1.59)	50-2.23 (2.32-2.22)	50-1.95 (2.02-1.95)
R_{sym} or R_{merge}	11.1% (72.1%)	13.1% (72.1%)	13.0% (70.0%)
$I / \sigma I$	19.6 (3.2)	18.0 (4.14)	27.5 (4.3)
Completeness (%)	96.0(100.0)	96.1(100.0)	100.0 (100.0)
Redundancy	7.3 (7.3)	7.2 (7.2)	9.2 (9.1)
Refinement			
Resolution (Å)	50-1.59	50-2.227	
No. reflections	87603	32409	
R_{work} / R_{free}	19.3%/23.8%	19.58%/25.24%	
No. atoms			
Protein	5,920	5,488	
Ligand/ion		2	
Water	446	159	
B-factors			
Protein	25.46	31.59	
Ligand/ion		30.71	
Water	31.30	31.39	
R.m.s deviations			
Bond lengths (Å)	0.017	0.008	
Bond angles (°)	1.810	0.999	

Only one crystal used to identify the structure of SspB. Values in parentheses are for the highest-resolution shell.

Table S2. Strains, plasmids and phages used in this study

Strain, plasmid and phage	Characteristics	Source or reference
Vibrio		
V. breoganii 1C-10	d(C_{PS}C), GenBank: AKXW00000000	[17]
V. breoganii ZF29	d(C_{PS}C), GenBank: AJYM00000000	[17]
V. cyclitrophicus FF75	d(C_{PS}C), GenBank: ATLT01000000	[17]
V. tasmaniensis 1F-267	d(G_{PS}A), d(G_{PS}T), GenBank: AJZO02000000	[17]
Streptomyces		
S. clavuligerus ATCC 27064	d(C_{PS}C), GenBank: CP027858	ATCC
S. yokosukanensis DSM 40224	d(C_{PS}C), GenBank: LMWN01000000	DSMZ
S. lividans HXY6	*S. lividans* 1326 derivative lacking *dnd* and *ssp* genes	[18]
E. coli		
Trans1-T1	F^- φ80(*lacZ*)ΔM15 Δ*lac*X74 *hsdR*($r_k^-m_k^+$) Δ*recA1398endA1 tonA*	TransGen Biotech
DH10B	F^- *mcrA* Δ(*mrr-hsdRMS-mcrBC*) φ80*dlacZ*ΔM15 Δ*lacX74 recA1* endA1 araD139 Δ (ara, leu)7697 *galU galK rpsL nupG* λ^-	Invitrogen
BL21(DE3)	F^- *ompT gal dcm lon hsdS*$_B$($r_B^-m_B^-$) λ(DE3 [*lacI lacUV5*-T7p07 *ind*1 *sam*7 *nin*5]) [*mal*B^+]$_{K-12}$(λ^S)	Novagen
3234/A	d(C_{PS}C), GenBank: LCVH01000033	ATCC
WM3064	*thrB1004 pro thi rpsL hsdS lacZ*Δ*M15* RP4-1360 Δ*(araBAD)*567 Δ*dapA*1341::[*erm pir*]	William W. Metcalf, University of Illinois Urbana Champaign
Plasmids		
pUC19	Cloning vector, 2.7 kb, Amp^r	TransGen Biotech
pBluescript II SK(+)	Cloning vector, 3 kb, Amp^r	[19]
pACYC184	Cloning vector, 4 kb, Cm^r	[20]
pEASY-Blunt Zero	Cloning vector, 3.9 kb, Amp^r, Kan^r	TransGen Biotech
pSET152	*E. coli-Streptomyces* shuttle vector, *aac(3)*IV, ColEI, *att*$^{\phi C31}$, *ori* T	[21]
pJC4	pWM91 derivative, Δ*uidA3::pir+, sacB*, Cm^r	[22]
pWHU732	pBluescript II SK(+) derivative with a 5.8-kb KpnI–BamHI fragment carrying *sspBCD* and a 1.8-kb SacII-XbaI fragments carrying *sspA* from *V. cyclitrophicus* FF75, d(C_{PS}C)	This work
pWHU733	pACYC184 derivative with a 3.4 kb XbaI-SphI fragment carrying *sspE* from *V. cyclitrophicus* FF75	This work
pWHU734	pEASY-Blunt Zero derivative with an engineered 3.1 kb *sspE* with 6×his tag at C-terminal	This work
pWHU735	pACYC184 derivative expressing *sspE* from *S. yokosukanensis* DSM 40224 under the PQL25 promoter	This work

pWHU1811	pSET152 derivative with a 7.1 kb XbaI-StuI fragment carrying *sspABCD* (GenBank accession no. SSCG_01551-SSCG_01548) homologs from *S. clavuligerus* ATCC 27064	This work
pWHU3261	Derivative of pWHU3641, expressing $SspE_{H639A}$	This work
pWHU3262	pWHU735 derivative expressing $SspE_{G97A}$ from *S. yokosukanensis* DSM 40224 under the PQL25 promoter	This work
pWHU3263	pWHU735 derivative expressing $SspE_{H639A}$ from *S. yokosukanensis* DSM 40224 under the PQL25 promoter	This work
pWHU3264	pET28a derivative containing *sspC* from *V. cyclitrophicus* FF75, expression vector	This work
pWHU3481	pBluescript II SK(+) derivative with a 5.8-kb KpnI–BamHI fragment carrying *sspBCD* and a 1.8-kb SacII-XbaI fragments carrying $sspA_{C314S}$ from *V. cyclitrophicus* FF75	This work
pWHU3603	pET28a derivative containing *sspB* from *S. clavuligerus* ATCC 27064, expression vector	This work
pWHU3640	pBluescript II SK(+) derivative with an 8-kb fragment carrying *sspBCDE* from *E. coli* 3234/A	This work
pWHU3641	pET28a derivative containing *sspE* from *S. yokosukanensis* DSM 40224, expression vector	This work
pWHU3642	pWHU3641 derivative expressing $SspE_{G97A}$, expression vector	This work
pWHU3643	pWHU3641 derivative expressing $SspE_{R100A}$, expression vector	This work
pWHU3644	pWHU3603 derivative expressing $SspB_{R23A}$, expression vector	This work
pWHU3645	pWHU3603 derivative expressing $SspB_{E204R}$, expression vector	This work
pWHU3646	pWHU3603 derivative expressing $SspB_{Y103A/E204R}$, expression vector	This work
pWHU3647	pWHU3603 derivative expressing $SspB_{F24R/Y103A}$, expression vector	This work
pWHU3648	pET28a derivative expressing SspA from *V. cyclitrophicus* FF75, expression vector	This work
pWHU3649	pET28a derivative expressing SspD from *V. cyclitrophicus* FF75, expression vector	This work
pWHU3654	pWHU1811 derivative expressing $SspAB_{R23A}CD$	This work
pWHU3655	pWHU1811 derivative expressing $SspAB_{E204R}CD$	This work
pWHU3656	pWHU1811 derivative expressing $SspAB_{Y103A/E204R}CD$	This work
pWHU3657	pWHU1811 derivative expressing $SspAB_{F24R/Y103A}CD$	This work
pWHU3658	pSET52 derivative with a 9.7-kb fragment carrying *sspABCDE* from *S. yokosukanensis* DSM 40224	This work
pWHU3659	pWHU3658 derivative expressing $SspABCDE_{G97A}$	This work
pWHU3660	pWHU3658 derivative expressing $SspABCDE_{R100A}$	This work
pWHU3661	pWHU3658 derivative expressing $SspABCDE_{H639A}$	This work

pWHU3314	pWHU3603 derivative expressing $SspB_{E18R}$, expression vector	This work
Phages		
JXY1	*Podoviridae*, lytic, dsDNA, 2,004 5'-CCA-3' in genome	This work
T4	*Myoviridae*, lytic, dsDNA, 4,476 5-CCA-3' in genome	[23]
T4gt	*Myoviridae*, lytic, dsDNA, 4,414 5-CCA-3' in genome	[24]
T1	*Siphoviridae*, lytic, dsDNA, 1,319 5-CCA-3' in genome	[23]
JMPW1	*Siphoviridae*, lytic, dsDNA, 1,355 5-CCA-3' in genome	[25]
JMPW2	*Siphoviridae*, lytic, dsDNA, 1,359 5-CCA-3' in genome	[25]
T5	*Siphoviridae*, lytic, dsDNA, 3,523 5-CCA-3' in genome	[23]
T7	*Podoviridae*, lytic, dsDNA, 1,444 5-CCA-3' in genome	[23]
EEP	*Siphoviridae*, lytic, dsDNA, 1,573 5-CCA-3' in genome	[26]
ϕX174	*Bullavirinae*, lytic, ssDNA, 59 5-CCA-3' in genome	[27]

Table S3. Primers and DNA sequences used in this study

Primers	Sequences
Construction of in-frame deletion mutants	
1907L1	GACTAGTCCTAGGTTCGCTTTCGTCAAA
1907L2	CGGTAACGACTTTCTGTTTGACCAATGCCTAACGGACAACACCA
1907R1	TGGTGTTGTCCGTTAGGCATTGGTCAAACAGAAAGTCGTTACCG
1907R2	TCCGAGCTCCATCTAGTGTTGCATTCCAGAA
1908L1	GACGAGTCCTCGCTGGTTCTTCAACTACTT
1908L2	GATGTGGTCGTATCTTGGCTTTGAGCTGTGCCGTGATAGA
1908R1	TCTATCACGGCACAGCTCAAAGCCAAGATACGACCACATC
1908R2	TCCGAGCTCCTCCAGCACGCTTAATACCA
1909L1	GCTCTAGAGGTGAGGAGTTATTAGCGATGT
1909L2	TTCTCCGTTATCACTTGTCTCTACTTGACCATTATCCACTTGTC
1909R1	GACAAGTGGATAATGGTCAAGTAGAGACAAGTGATAACGGAGAA
1909R2	TCCGAGCTCAACACATTTGCCCTCAATCTG
1910L1	GACTAGTCTCAACTACTCCAAGAGCATA
1910L2	TCAGATATGGTTTAGAGCGACAACCTAAATTCGTATAGCG
1910R1	CGCTATACGAATTTAGGTTGTCGCTCTAAACCATATCTGA
1910R2	TCCGAGCTCAGTGACGAATACAGTTGAGT
1902L1	GGACTAGTCGAGATGACGCTATTGAGTTG
1902L2	ACATAGCATTACACGCCGAAGCACCGCAGGTAAATACAA
1902R1	TTGTATTTACCTGCGGTGCTTCGGCGTGTAATGCTATGT
1902R2	TCCGAGCTCGGAGCCATTAAAGCGTGATAT
1906-1903L1	GGACTAGTAATGCCTAACGGACAACAC
1906-1903L2	AACCATAAGCACATCTCCACAAATGTCATAACCTCGCCTAG
1906-1903R1	CTAGGCGAGGTTATGACATTTGTGGAGATGTGCTTATGGTT
1906-1903R2	TCCGAGCTCCGTTCCTAGCTCATTGTTCAC
1907-1909L1	GAGCTCCTAGGTTCGCTTTCGTCAAA
1907-1909L2	TTATCACTTGTCTCCCAATGCCTAACGGA
1907-1909R1	TCCGTTAGGCATTGGGAGACAAGTGATAA
1907-1909R2	GAGCTCATTTGCCCTCAATCTG
1910-BCD-L1	CGAGCTC GCAGATAGTGCTCCGATCAATA
1910-BCD-L2	TCACAAACTCAGGACTCCAACTTTTGGCATCACCGCTATATACA
1910-BCD-R1	TGTATATAGCGGTGATGCCAAAAGTTGGAGTCCTGAGTTTGTGA
1910-BCD-R2	CGAGCTCTAGCGAACGACACCCTGAAA
Plasmid construction	
sspBCD-1	CGGGATCCAGCAGCTTGATACCATGAGATT
sspBCD-2	GGGGTACCTTGGAATGCCGATGTTAAGC
sspA-1	GCTCTAGAGGAGAACATAATCGGTCTACCA
sspA-2	TCCCCGCGGCACTACTGCTGCGAGTCTAC
184sspE-1	GCTCTAGATTCCACTCTACGGTAACCTCTC
184sspE-2	ACATGCATGCCCAGAACGAATCGCACAGATAA
sspE-2-his	CTAGTGGTGATGATGGTGATGTACGAATTTAGGTTGAATACTC
sspA-L1	GGAGAACATAATCGGTCTACCA
sspA-L2	TAGCATTAGACGCCGAGCCTTGGGATAT
sspA-R1	CTCGGCGTCTAATGCTATGTCTAACACA
sspA-R2	CACTACTGCTGCGAGTCTAC
40224e-F-pql25	TTAAAGAGGAGAAAGGTACCATGGAGACTAAAGAGATCTTCG
40224e-R-pql25	CGCCCCCCTGAGTTTTCGTTACGGCTCGAATCCCAGCC
pql25-F-40224e	TTCCACTCTACGGTAACCTCTCCATTTTAGTGGTGGGAGTTG
pql25-R-40224e	CGAAGATCTCTTTAGTCTCCATGGTACCTTTCTCCTCTTTAA
733-F-pql2540224e	GGCTGGGATTCGAGCCGTAACGAAAACTCAGGGGGGCG

733-R-40224epql25	CAACTCCCACCACTAAAATGGAGAGGTTACCGTAGAGTGGAA

DNA substrates of SspE from T4 genome

0CC-1	CTTTATTTTACTTGAATTGTGC
0CC-2	GAAAATTATGTTAGCTTATCAAGCACG
1CC-1	GCGTTCAGCTCTTTGCTTTTTGTA
1CC-2	GATAAAGCATCTAAATTATCTCG
1CCA-1	CAAACATTAAATTTTCCTCGCTAA
1CCA-2	ATGTTAAAGTTGTCATTCAAGAA

SspB protein expression in pWHU3603

pET28a-sspB-1	GATCAACGCCATATGATGTCAGACAGTCGGCTCG
pET28a-sspB-2	GATCAACGCAAGCTTTCACACGGTCTCCTCGG
sspB-E18R-1	CGCGCGCCACGGGACCTTCGCG
sspB-E18R-2	CGCGAAGGTCCCGTGGCGCGCG
sspB-R23A-1	TCGCGCCGGCCTTCGGGTGGCTCCA
sspB-R23A-2	CACCCGAAGGCCGGCGCGAAGGTCT
sspB-F24R-1	GCGCCGCGCGCCGGGTGGCTCCACA
sspB-F24R-2	GCCACCCGGCGCGCGGCGCGAAGGT
sspB-Y103A-1	GCCGACCCCGCCCTGGAAGAGCTCG
sspB-Y103A-2	CTTCCAGGGCGGGGTCGGCTCCATC
sspB-E204R-1	CCATCAGCCCGAGCCGACGGAACGG
sspB-E204R-2	CCGTTCCGTCGGCTCGGGCTGATGG

SspE protein expression in pWHU3641

pET28a-sspE-1	GGGAATTCCATATGATGGAGACTAAAGAGATCTTCG
pET28a-sspE-2	ATAAGAATGCGGCCGCTTACGGCTCGAATCCCAG
sspE-G97A-1	TCATCGACGCTCAGCAGAGGATGACCACACTTCTCC
sspE-G97A-2	TCTGCTGAGCGTCGATGATAGTCATCACCTTGGAGG
sspE-R100A-1	GGTCAGCAGGCGATGACCACACTTCTCCTATTGACGACCGTTTT
sspE-R100A-2	TGTGGTCATCGCCTGCTGACCGTCGATGATAGTCATCACCTT
sspE-H639A-1	CGCCACTATCGAAGCCGTAGCTCCTCAGG
sspE-H639A-2	CCTGAGGAGCTACGGCTTCGATAGTGGCG

SspA protein expression in pWHU3648

pET28a-sspA-1	CATATGATGACTAAGTATTTCGATTACG
pET28a-sspA-2	CTCGAGCTACACTTTATAAGGAGGTAAGC

SspC protein expression in pWHU3264

pET28a-sspC-1	CATGCCATGGGCATGACACTAGCCAATCAA
pET28a-sspC-2	ACGCGTCGACACCTTGAGCTTCCAATGCT

SspD protein expression in pWHU3649

pET28a-sspD-1	CCTGGTGCCGCGCGGCAGCCATATGATGGCTAGGGAGTACCCAG
pET28a-sspD-2	GGTGGTGGTGGTGCTCGAGTGCGGCCGCCTATTTGTAACAAGTTACAC

Quantitative RT-PCR

q-sspBCD-1	AATGGCGTGCGAAGTGAT
q-sspBCD-2	TTCTGCCCAAGCGTGTCC
q-sspE-1	ACGTTTAACCCAAGTCCGCT
q-sspE-2	AACGACGGTAGTGGGAGAGA
q-gapdh-1	CAGCTGAGCGTAACCCAGAA
q-gapdh-2	AGATGCTTGGTTAACGCCCA

dsDNA used in NTPase activity assay

CCA	5’-TGTGGCAAAGAATCTATTGCCAGAAGCCAGTTTCGATACT-3’
	3’-ACACCGTTTCTTAGATAACGGTCTTCGGTCAAAGCTATGA-5’
C_{PS}CA	5’-TGTGGCAAAGAATCTATTGC$_{PS}$CAGAAGCCAGTTTCGATACT-3’
	3’-ACACCGTTTCTTAGATAACGGTCTTCGGTCAAAGCTATGA-5’
GAAC	5’-TGTGGCAAAGAATCTATTGGAACAAGCCAGTTTCGATACT-3’
	3’-ACACCGTTTCTTAGATAACCTTGTTCGGTCAAAGCTATGA-5’
G_{PS}AAC	5’-TGTGGCAAAGAATCTATTGG$_{PS}$AACAAGCCAGTTTCGATACT-3’
	3’-ACACCGTTTCTTAGATAACCTTGTTCGGTCAAAGCTATGA-5’
GTTC	5’-TGTGGCAAAGAATCTATTGGTTCAAGCCAGTTTCGATACT-3’
	3’-ACACCGTTTCTTAGATAACCAAGTTCGGTCAAAGCTATGA-5’
G_{PS}TTC	5’-TGTGGCAAAGAATCTATTGG$_{PS}$TTCAAGCCAGTTTCGATACT-3’
	3’-ACACCGTTTCTTAGATAACCAAGTTCGGTCAAAGCTATGA-5’
GGCC	5’-TGTGGCAAAGAATCTATTGG$_{PS}$GCCAAGCCAGTTTCGATACT-3’
	3’-ACACCGTTTCTTAGATAACCCGGTTCGGTCAAAGCTATGA-5’
G_{PS}GCC	5’-TGTGGCAAAGAATCTATTGG$_{PS}$GCCAAGCCAGTTTCGATACT-3’
	3’-ACACCGTTTCTTAGATAACCCGGTTCGGTCAAAGCTATGA-5’

Table S4. SspE structural data collection and refinement statistics

	Selenomethionine-substituted SspE
Data collection	
Space group	$P2_12_12_1$
Cell dimensions	
a, *b*, *c* (Å)	*a*=111.07 Å, *b*=138.16 Å, *c*=293.68 Å,
α, β, γ (°)	α=β=γ=90°
Wavelength	0.97893 Å
Resolution (Å)	125.02-3.31 (3.43-3.31)
R_{sym} or R_{merge}	14.0% (190.3%)
$I / \sigma I$	8.58 (1.5)
Completeness (%)	99.50 (96.27)
Redundancy	6.9 (6.3)
Refinement	
Resolution (Å)	125.02-3.31
No. reflections	128,999
R_{work} / R_{free}	34.77/39.77
No. atoms	
Protein	15028
Ligand/ion	
Water	
B-factors	
Protein	113.63
Ligand/ion	
Water	
R.m.s deviations	
Bond lengths (Å)	0.013
Bond angles (°)	1.464

Only one crystal was used to identify the structure of SspE. Values in parentheses are for the highest-resolution shell.

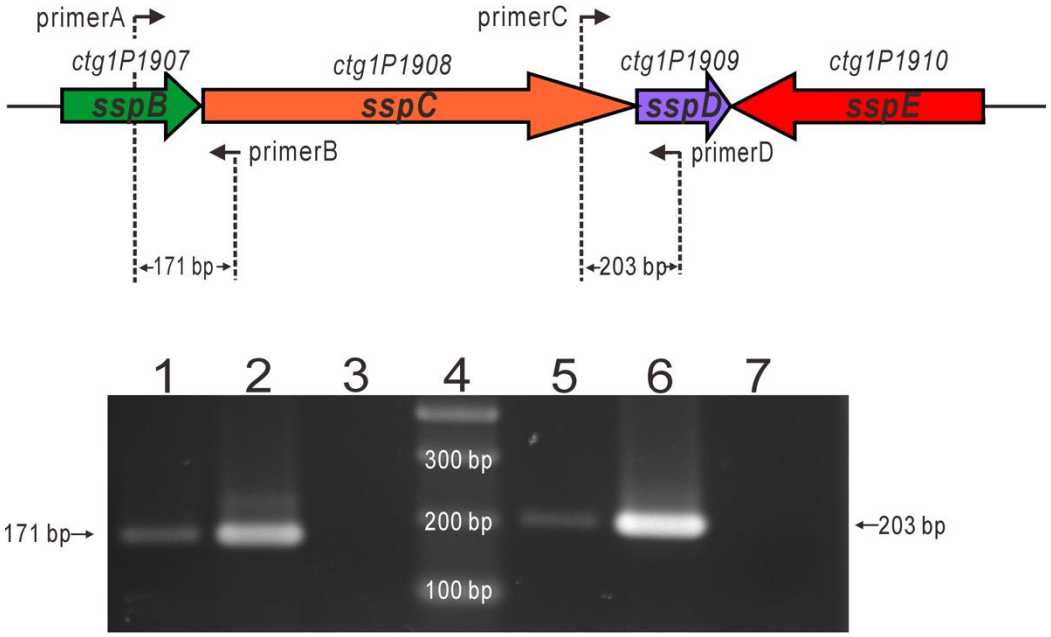

Figure S1. RT-PCR analysis of the cotranscription of *M565_ctg1P1907* to *M565_ctg1P1909* (*sspBCD*). Primers are schematically shown above or below the genes. PCR products were obtained using reverse-transcribed cDNA (lanes 1, 5), genomic DNA (lanes 2, 6) and nontranscribed RNA (lanes 3, 7) of *V. cyclitrophicus* FF75 as templates. Primer A (5'-TGCTGCTGAACGAGTAACTGAA-3') and primer B (5'-ACGGACGGCGATGGAGTATT-3') were used as the primer pair to produce PCR fragments of 171-bp, whereas primer C (5'-AAGAACAACTTGCCGCACTCAG-3') and primer D (5'-CAAGCTCTGGGTACTCCCTAGC-3') were used to generate 203 bp fragments. Lane 4, LD Marker 1 (Dongsheng Biotech, China). Results are representative of two independent experiments.

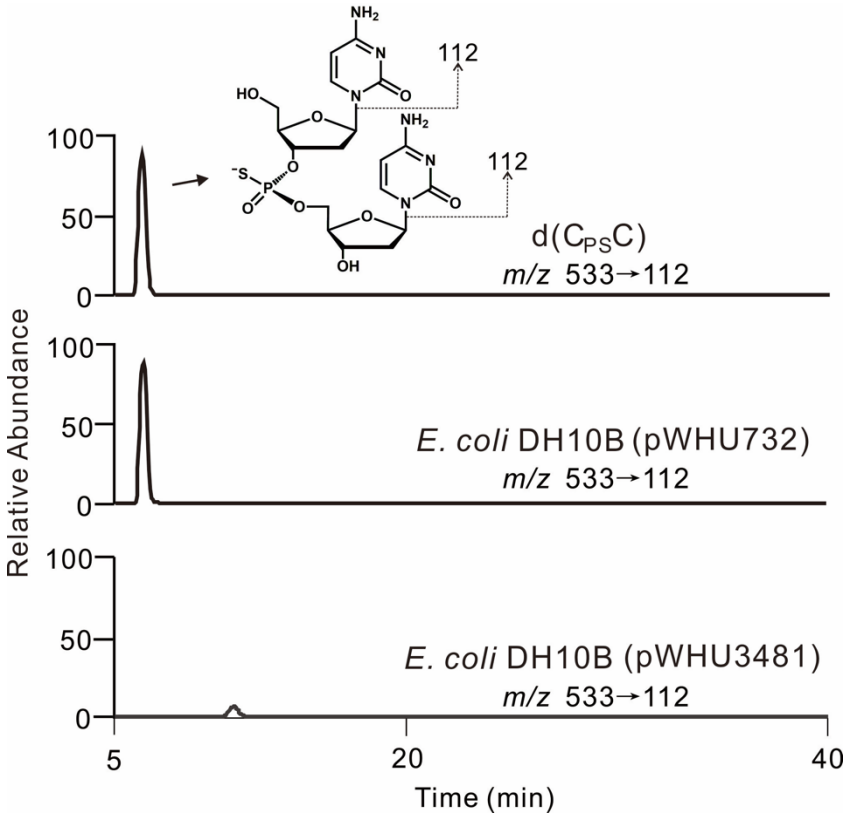

Figure S2. PT detection using liquid chromatography-tandem quadrupole mass spectrometry (LC-MS/MS). Plasmid pWHU732, expressing *M565_ctg1P1902* (*sspA*) and *M565_ctg1P1907* to *M565_ctg1P1909 (sspBCD)* from *V. cyclitrophicus* FF75, produced d(C_{PS}C) in *E. coli* DH10B. The single point mutation C314S in SspA in pWHU3481, possessing *sspA*$_{C314S}$*BCD*, abolished DNA PT modification in d(C_{PS}C). The fragmentation pattern of the d(C_{PS}C) standard is shown in the structural inset. Data are representative of three independent experiments.

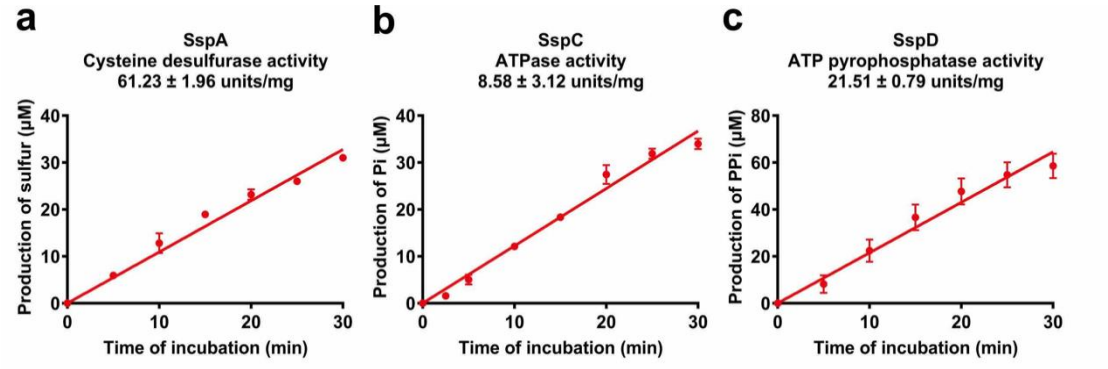

Figure S3. Enzymatic activity analysis of SspA, SspC and SspD from *V. cyclitrophicus* FF75. (**a**) SspA cysteine desulfurase activity was measured as sulfide production using L-cysteine as the substrate as described by Siegal *et al*[28]. The reaction was carried out at 28 °C in a solution containing 50 mM Tris-HCl (pH 8.0), 0.02 mM pyridoxal 5'-phosphate, 5 mM DTT, 10 mM L-cysteine and 500 nM SspA in a total volume of 200 μL. The reaction was quenched by adding 25 μL of 20 mM *N*, *N*-dimethyl-*p*-phenylenediamine sulfate in 7.2 M HCl and 25 μL of 30 mM $FeCl_3$ in 1.2 M HCl at the indicated time points, followed by a 30-min incubation in the dark at 28 °C. The absorption of the final product, methylene blue, was measured at 650 nm. A freshly prepared Na_2S solution was used as a standard to determine the concentration of sulfide. (**b**) An ATPase assay for SspC was performed with the QuantiChrom™ ATPase/GTPase Assay kit (BioAssay Systems) according to the manufacturer's instructions. Typically, the reaction was conducted at 28 °C in a solution containing 20 mM Tris, 40 mM NaCl, 4 mM $MgAc_2$, 0.5 mM EDTA, pH 7.5, 1 mM ATP and 1 μM SspC in a total volume of 40 μL for the indicated incubation times. The reaction was quenched by 200 μL of malachite green reagent, which can form a colorimetric complex with an absorbance maximum at 620 nm upon reaction with inorganic phosphates (Pi) liberated by enzymes. A standard curve was made using a 1 mM phosphate solution provided in the kit. (**c**) The ATP pyrophosphatase activity of SspD was analyzed by using an EnzCheck pyrophosphate assay kit (Molecular Probes), which contains an inorganic pyrophosphatase capable of transforming inorganic pyrophosphate (PPi) to Pi. In the presence of Pi, 2-amino-6-mercapto-7-methylpurine ribonucleoside (MESG) is converted enzymatically by purine nucleoside phosphorylase to ribose 1-phosphate and 2-amino-6-mercapto-7-methylpurine; the latter product has a characteristic UV absorption at 360 nm, allowing the detection of Pi released from ATP. The assay was conducted in a 200-μL reaction volume containing in 0.2 mM MESG, 0.2 U of purine nucleoside phosphorylase, 0.006 U of inorganic pyrophosphatase, 1 mM ATP and 3 μM SspD. The units were defined as the amount of protein required to catalyze the formation of 1 nmol of the product (sulfur, Pi or PPi) per minute. Data are shown as mean ± SD and are representative of three independent experiments. Error bars represent the SD of the means.

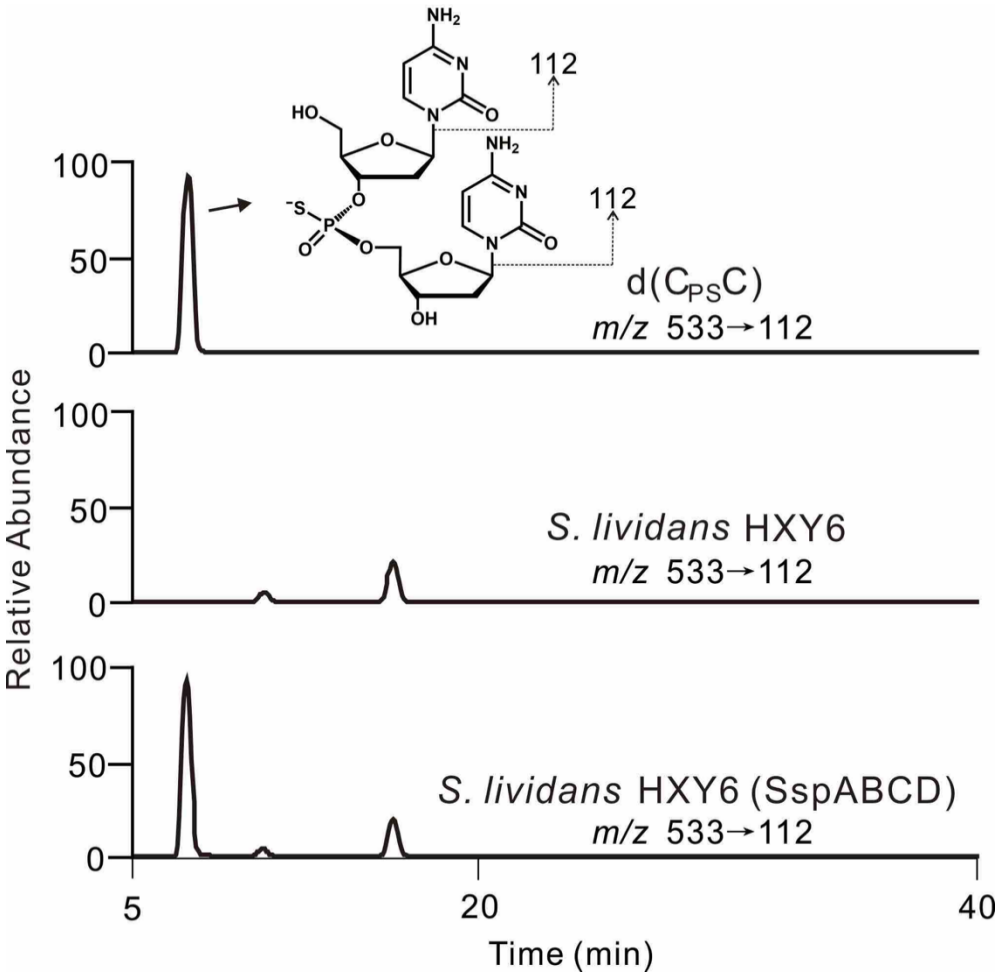

Figure S4. LC-MS/MS analysis of PT-modified d(C_{PS}C) in *S. lividans* HXY6. The heterologous expression of *sspABCD* from *S. clavuligerus* ATCC 27064 produced d(C_{PS}C) in *S. lividans* HXY6, which lacks endogenous *ssp* genes and PT modification. The fragmentation pattern of a d(C_{PS}C) standard is shown in the structural inset. Results are representative of three independent experiments.

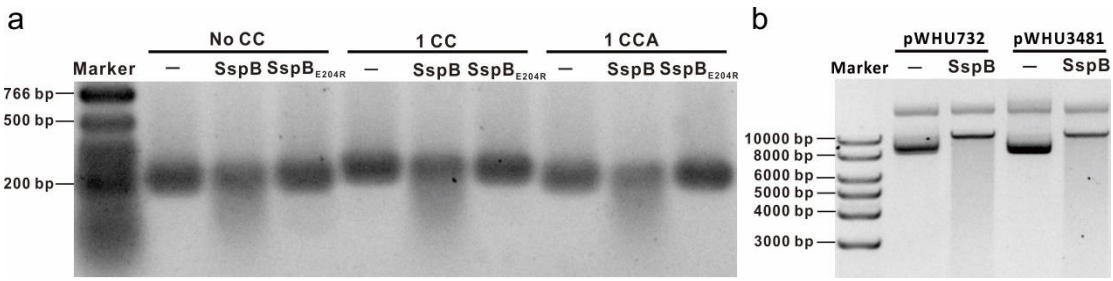

Figure S5. Alkaline-denaturing and neutral gel electrophoresis patterns of SspB- and SspB$_{E204R}$-treated DNA substrates. (a) Approximately 1 μg of different kinds of DNA substrates (with no 5'-CC-3', with one 5'-CC-3', and with one 5'-CCA-3') were incubated with 2 μM SspB or SspB$_{E204R}$ of *S. clavuligerus* ATCC 27064 at 28 °C for 9 h. Denatured DNA was analyzed on a 2% agarose gel under denaturing conditions. The DNA fragments with no 5'-CC-3', with one 5'-CC-3', and with one 5'-CCA-3' were PCR-amplified from the phage T4 genome using the primer pairs 0CC-1/0CC-2, 1CC-1/1CC-2 and 1CCA-1/1CCA-2 (Supplementary Table S3), respectively. (b) Three hundred nanograms of PT-modified pWHU732, carrying *sspABCD* or non-PT modified pWHU3481 carrying *sspA*$_{C314S}$*BCD*, were incubated with 2 μM SspB at 28 °C for 4 h, followed by electrophoresis on a 1% native agarose gel. Results in (a) and (b) are representative of three independent experiments.

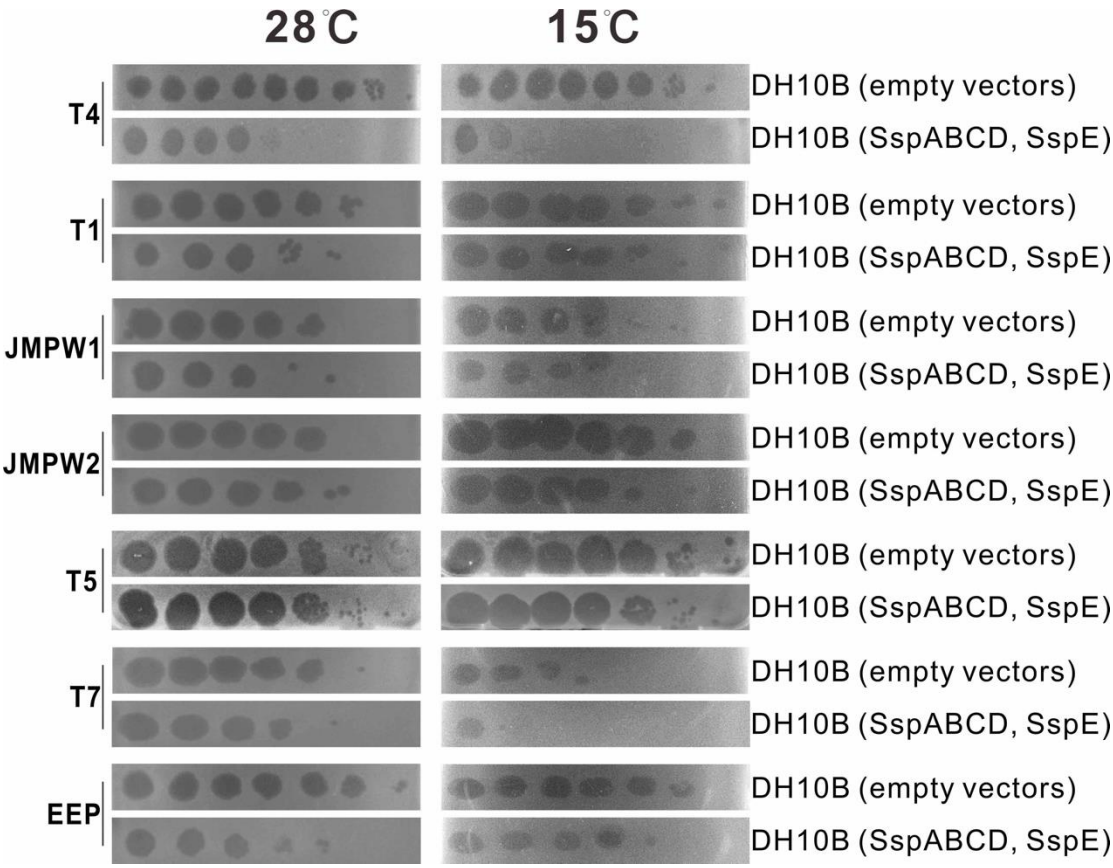

Figure S6. Thermoregulated anti-phage activity of SspABCD-SspE from *V. cyclitrophicus* FF75. Cell lawns of *E. coli* DH10B (empty vectors) and DH10B (SspABCD, SspE) were spotted with serial dilutions of phage lysates, followed by cultivation at 28 °C and 15 °C, respectively. Results are representative of two independent experiments.

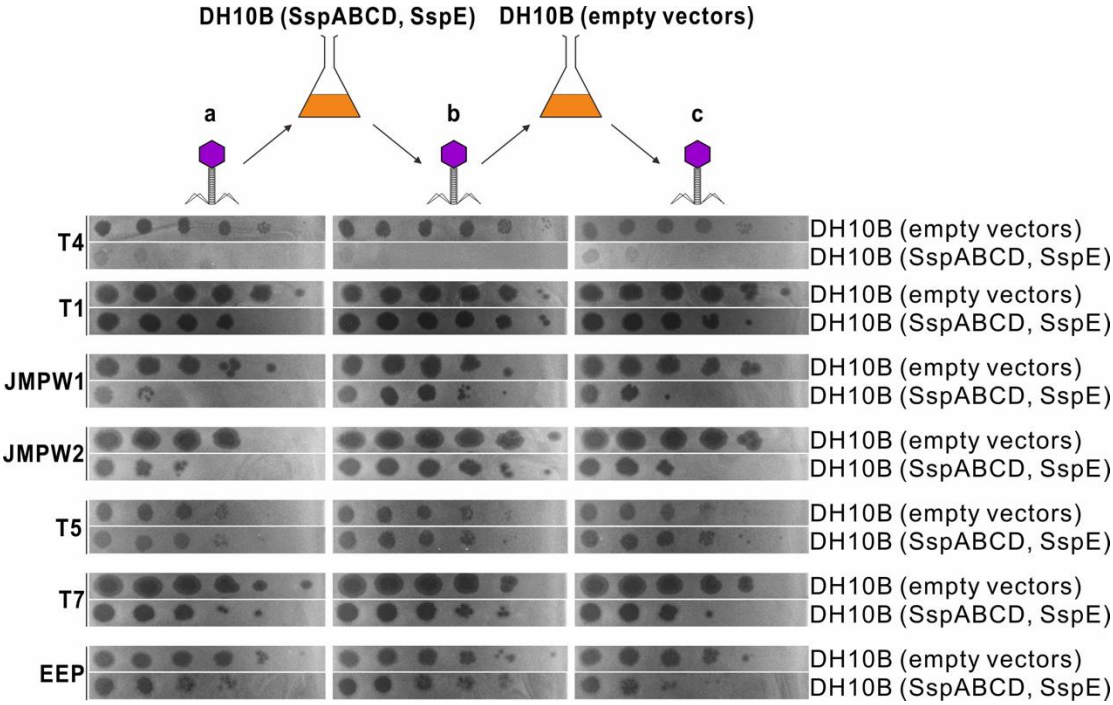

Figure S7. Restriction of phages by SspABCD-SspE. (**a**) Cell lawns of *E. coli* DH10B containing empty vectors or SspABCD-SspE of *V. cyclitrophicus* FF75 were spotted with the phages indicated on the left. Phages passaged through DH10B (SspABCD, SspE) (**b**) and then DH10B (empty vectors) (**c**) lacking the Ssp system were used to reinfect DH10B (SspABCD, SspE) and DH10B (empty vectors) cells, respectively, at 28 °C. Phage T4 propagated on DH10B (SspABCD, SspE) was still be sensitive to the Ssp defense, suggesting that T4 DNA may not be PT modified on 5'-CCA-3' due to the hindrance of glucosyl-hydroxymethylated cytosine. All results are representative of three independent experiments.

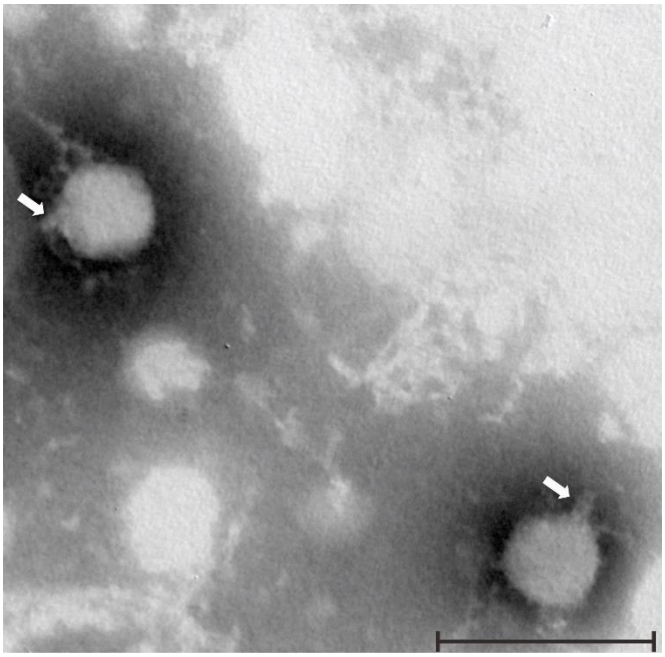

Figure S8. The morphology of phage JXY1. Electron microscopy of phage JXY1 isolated from soil samples on the campus of Wuhan University. The phage JXY1 has a spherical head with a diameter of 66.3 ± 2.7 nm and a short tail. JXY1 belongs to the *Podoviridae* family based on its morphological property of a short tail and high genomic homology with the *Podoviridae* family of phages. Scale bar, 0.1 μm. Results are representative of three independent experiments.

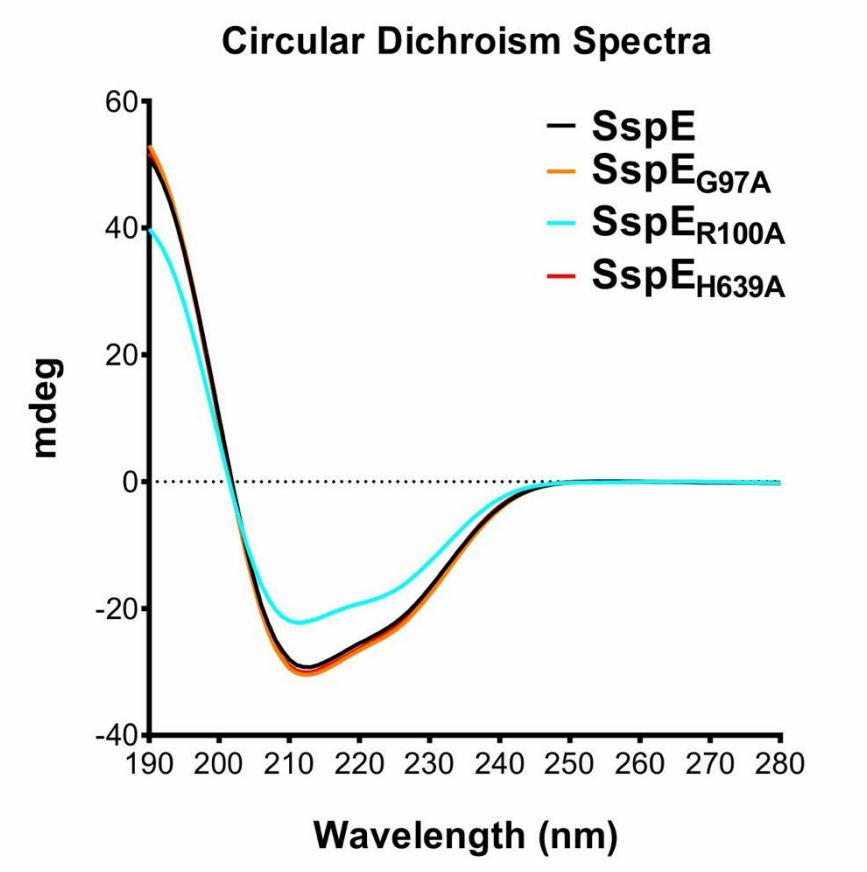

Figure S9. CD spectra of wild-type and variants SspE. The spectra of SspE$_{G97A}$ and SspE$_{H639A}$ are essentially identical to that of wild-type SspE. For SspE$_{R100A}$, the spectrum exhibited a decreased signal amplitude, indicating a structural perturbation or a global destabilization of the protein. Results are representative of two independent experiments.

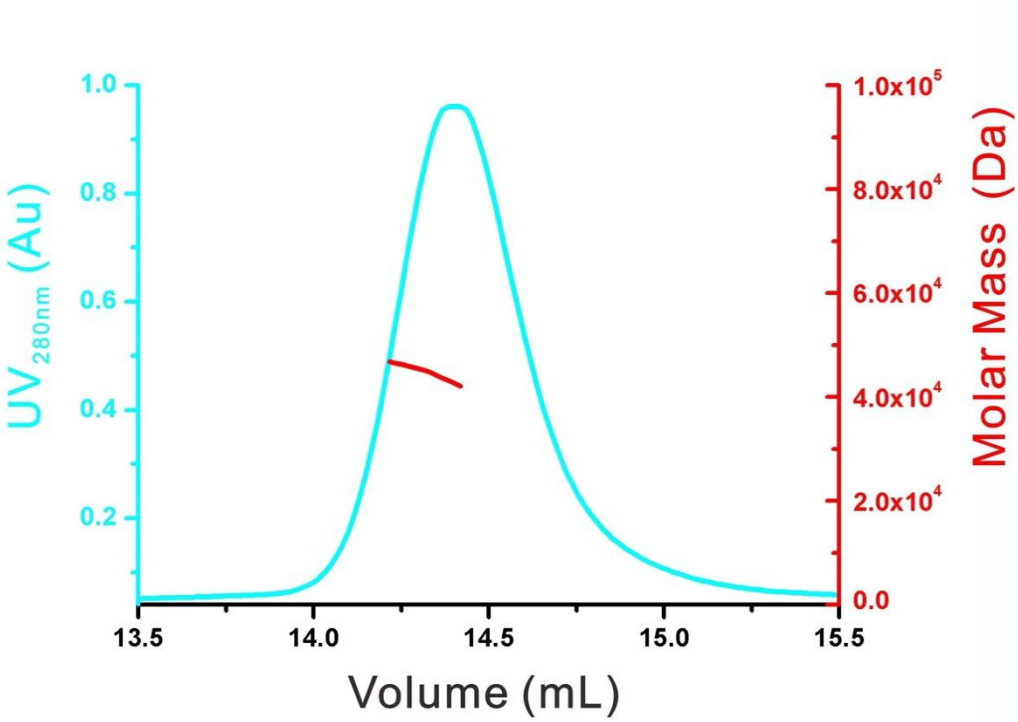

Figure S10. The SspB protein in solution behaves as a monomer, as assayed by the size-exclusion chromatography-multiangle static light scattering method. The blue line represents UV absorption at 280 nm (left axis, Au), while the red line represents the molecular mass (right axis, Da). Results are representative of two independent experiments.

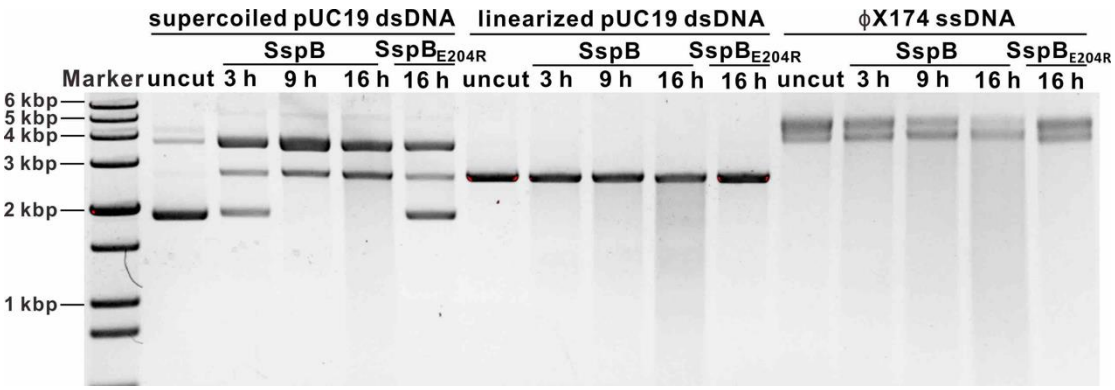

Figure S11. Assays of SspB nicking different forms of DNA. In these assays, 0.3 µg of supercoiled pUC19 dsDNA, BamHI-linearized pUC19 dsDNA, and ϕX174 ssDNA were untreated or treated with 2 µM SspB at 28 °C in CutSmart (New England Biolabs, 50 mM potassium acetate, 20 mM Tris-acetate, pH 7.9, 10 mM magnesium acetate, 1.5 µM BSA). At the indicated time points, aliquots of the reaction mixture were withdrawn and analyzed on a 1% agarose gel. Results are representative of two independent experiments.

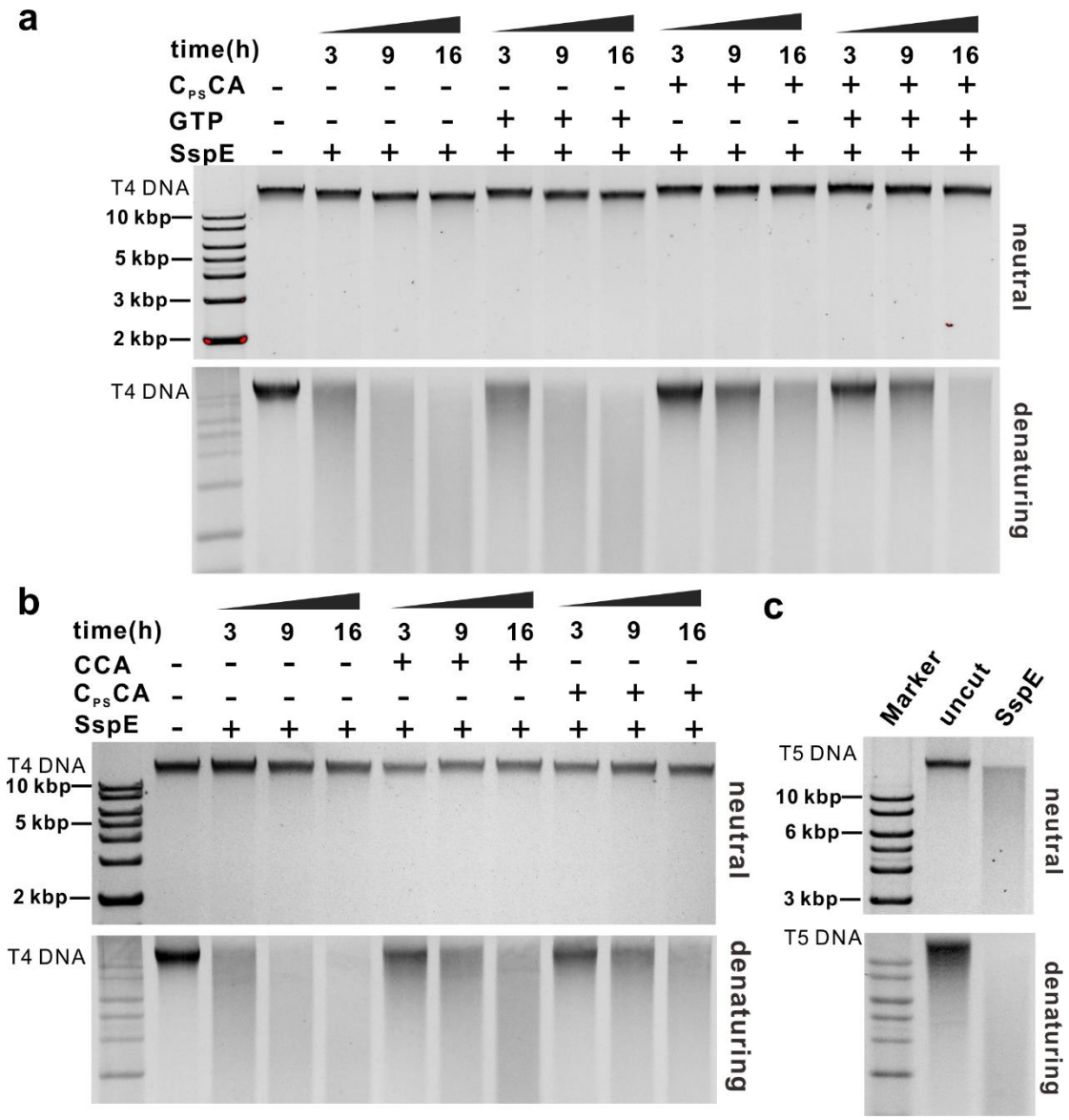

Figure S12. DNA nicking assays of SspE on phage DNA *in vitro*. (**a, b**) The effect of GTP and DNA containing the 5'-C_{PS}CA-3' or 5'-CCA-3' motif on the nicking endonuclease activity of SspE. The nicked products were analyzed on a native agarose gel and a denaturing alkaline gel. (**c**) Phage T5 DNA was susceptible to nicking damage by SspE *in vitro*. All images shown are representative of three independent experiments.

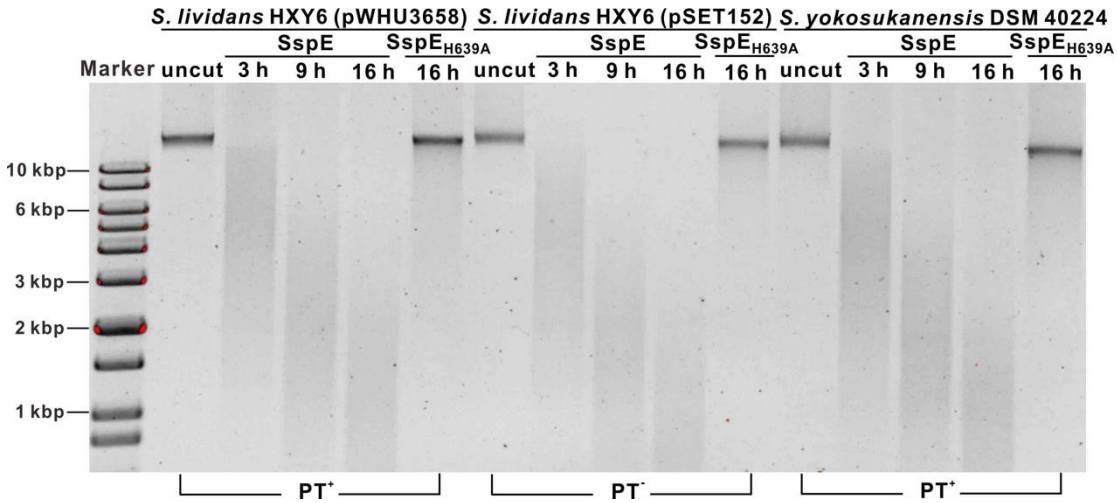

Figure S13. DNA nicking assay of SspE with bacterial genomic DNA. In this assay, 0.3 µg of genomic DNA isolated from PT-containing HXY6(pWHU3658) and DSM 40224 and from PT-lacking HXY6(pSET152) were treated with 2 µM SspE at 28 °C in CutSmart buffer. At the indicated time points, aliquots of the reaction mixture were withdrawn and analyzed on a 1% agarose gel. SspE$_{H639A}$-treated DNA was used as a control. Results are representative of two independent experiments.

Supplementary References

1. Wah, D.A., Bitinaite, J., Schildkraut, I. & Aggarwal, A.K. Structure of FokI has implications for DNA cleavage. *Proc Natl Acad Sci U S A* **95**, 10564-9 (1998).
2. Cao, B. et al. Pathological phenotypes and *in vivo* DNA cleavage by unrestrained activity of a phosphorothioate-based restriction system in *Salmonella*. *Mol Microbiol* **93**, 776-85 (2014).
3. Gan, R. et al. DNA phosphorothioate modifications influence the global transcriptional response and protect DNA from double-stranded breaks. *Sci Rep* **4**, 6642 (2014).
4. Xiong, L. et al. A new type of DNA phosphorothioation-based antiviral system in archaea. *Nat Commun* **10**, 1688 (2019).
5. Zhang, Y. & Skolnick, J. TM-align: a protein structure alignment algorithm based on the TM-score. *Nucleic Acids Res* **33**, 2302-9 (2005).
6. Machnicka, M.A., Kaminska, K.H., Dunin-Horkawicz, S. & Bujnicki, J.M. Phylogenomics and sequence-structure-function relationships in the GmrSD family of Type IV restriction enzymes. *BMC Bioinformatics* **16**, 336 (2015).
7. Bair, C.L. & Black, L.W. A type IV modification dependent restriction nuclease that targets glucosylated hydroxymethyl cytosine modified DNAs. *J Mol Biol* **366**, 768-78 (2007).
8. Hoyland-Kroghsbo, N.M., Munoz, K.A. & Bassler, B.L. Temperature, by Controlling Growth Rate, Regulates CRISPR-Cas Activity in *Pseudomonas aeruginosa*. *MBio* **9**(2018).
9. O'Driscoll, J. et al. Lactococcal plasmid pNP40 encodes a novel, temperature-sensitive restriction-modification system. *Appl Environ Microbiol* **70**, 5546-56 (2004).
10. Kim, J.W. et al. A novel restriction-modification system is responsible for temperature-dependent phage resistance in *Listeria* monocytogenes ECII. *Appl Environ Microbiol* **78**, 1995-2004 (2012).
11. Li, J. et al. Quantitative mapping of DNA phosphorothioatome reveals phosphorothioate heterogeneity of low modification frequency. *PLoS Genet* **15**, e1008026 (2019).
12. Cao, B. et al. Genomic mapping of phosphorothioates reveals partial modification of short consensus sequences. *Nat Commun* **5**, 3951 (2014).
13. Xia, S. et al. Tight control of genomic phosphorothioate modification by the ATP-modulated autoregulation and reusability of DndB. *Mol Microbiol* (2018).
14. McCorquodale, D.J. & Warner, H.R. Bacteriophage T5 and Related Phages. in *The Bacteriophages* (ed. Calendar, R.) 439-475 (Springer US, Boston, MA, 1988).
15. Davison, J. & Brunel, F. Restriction insensitivity in bacteriophage T5. II. Lack of EcoRI modification in T5+ and T5ris mutants. *J Virol* **29**, 17-20 (1979).
16. Wang, J. et al. Complete genome sequence of bacteriophage T5. *Virology* **332**, 45-65 (2005).

17. Cordero, O.X. et al. Ecological populations of bacteria act as socially cohesive units of antibiotic production and resistance. *Science* **337**, 1228-31 (2012).
18. Liang, J. et al. DNA modification by sulfur: analysis of the sequence recognition specificity surrounding the modification sites. *Nucleic Acids Res* **35**, 2944-54 (2007).
19. Alting-Mees, M.A. & Short, J.M. pBluescript II: gene mapping vectors. *Nucleic Acids Res* **17**, 9494 (1989).
20. Chang, A.C. & Cohen, S.N. Construction and characterization of amplifiable multicopy DNA cloning vehicles derived from the P15A cryptic miniplasmid. *J Bacteriol* **134**, 1141-56 (1978).
21. Bierman, M. et al. Plasmid cloning vectors for the conjugal transfer of DNA from *Escherichia coli* to *Streptomyces spp*. *Gene* **116**, 43-9 (1992).
22. Metcalf, W.W. et al. Conditionally replicative and conjugative plasmids carrying *lac*Z alpha for cloning, mutagenesis, and allele replacement in bacteria. *Plasmid* **35**, 1-13 (1996).
23. Demerec, M. & Fano, U. Bacteriophage-Resistant Mutants in *Escherichia Coli*. *Genetics* **30**, 119-36 (1945).
24. Georgopoulos, C.P. Isolation and preliminary characterization of T4 mutants with nonglucosylated DNA. *Biochem Biophys Res Commun* **28**, 179-84 (1967).
25. Shen, M. et al. Complete Genome Sequences of T1-Like Phages JMPW1 and JMPW2. *Genome Announc* **4**(2016).
26. Li, S. et al. Characterization and genome sequencing of a novel coliphage isolated from engineered *Escherichia coli. Intervirology* **53**, 211-20 (2010).
27. Tessman, I. Some unusual properties of the nucleic acid in bacteriophages S13 and phi X174. *Virology* **7**, 263-75 (1959).
28. Siegel, L.M. A Direct Microdetermination for Sulfide. *Anal Biochem* **11**, 126-32 (1965).